Medical Devices: Evidence and Research

Dovepress
open access to scientific and medical research

Open Access Full Text Article

ORIGINAL RESEARCH

Metered Cryospray™: a novel uniform, controlled, and consistent in vivo application of liquid nitrogen cryogenic spray

This article was published in the following Dove Press journal:
Medical Devices: Evidence and Research
17 February 2017
Number of times this article has been viewed

Thomas I Mulcahey[1]
James E Coad[2]
Wei Li Fan[1]
Daniel J Grasso[1]
Brian M Hanley[1]
Heather V Hawkes[1]
Sean A McDermott[1]
John P O'Connor[1]
Ellen E Sheets[1]
Charles J Vadala[1]

[1]CSA Medical Inc., Lexington, MA, [2]Pathology Laboratory for Translational Medicine, West Virginia University, Morgantown, WV, USA

Video abstract

Point your SmartPhone at the code above. If you have a QR code reader the video abstract will appear. Or use: http://youtu.be/mgp5_k-VHyM

Correspondence: John P O'Connor
CSA Medical Inc., 91 Hartwell Avenue, Lexington, MA 02421, USA
Tel +1 781 538 4755
Fax +1 781 538 4730
Email joconnor@csamedical.com

Abstract: In this article, a novel cryotherapy approach using a uniform, controlled, and consistent in vivo application of liquid nitrogen (LN_2) spray as a Metered Cryospray™ (MCS) process is described. Although MCS may be used for many potential clinical applications, this paper focuses on the development that led to the controlled and consistent delivery of radial LN_2 cryogen spray in order to generate a uniform circumferential effect and how the amount of MCS can be adapted to specifically ablate targeted diseases within a patient's lumen such as an airway or esophagus.

Keywords: Metered Cryospray™, cryoablation, rejuvenative healing, LN_2 spray cryotherapy

Introduction

For several decades, cryogenic freezing and regenerative healing have been used by dermatologists.[1–4] Since the first medical use of liquid nitrogen (LN_2) on external body surfaces, a significant number of peer-reviewed medical articles on its cryothermic use have been published.[5] These applications often incorporate the spraying of LN_2 or other cryogen on a skin feature, for example, a mole, to ablate the feature with a subsequent regenerative or rejuvenative healing process with little or no scarring.

More recently, cryogenic ablation of lesions and diseases has transitioned to within the body (eg, Liapi and Geschwind[6]). Common approaches include the use of a cryoprobe[7] or needle[8,9] that is placed into direct contact with the targeted tissue. These cryoprobes commonly use a compressed gas, such as argon, nitrous oxide, or carbon dioxide, which is allowed to rapidly expand into an enclosed volume, typically the tip of the cryosurgical unit. By the Joule–Thomson (J-T) effect,[10] the temperature of the compressed gas drops significantly and freezes the adjacent tissue; −40°C to −89°C have been routinely achieved with these devices, whereas some LN_2-based cryoneedles achieve −160°C. The J-T process enables such cryogens to ablate various tissues ranging from benign to malignant and drives slow freezing of the targeted tissue over a period of several to 10s of minutes. Initial cooling from normal body temperature to 0°C slows the cellular metabolism.[11] As the cooling continues from 0°C to −20°C, ice crystals begin to form in the extracellular environment. As a result, free intracellular water is osmotically pulled from the cells and into the partially frozen extracellular medium, resulting in cellular dehydration and shrinkage. This may also cause cellular death due to dehydration effects (Figure 1).

Unlike other cryogen devices that hold the cryogen within a contained probe or a needle, CSA Medical Inc. has pioneered the use of an LN_2 spray within the body to

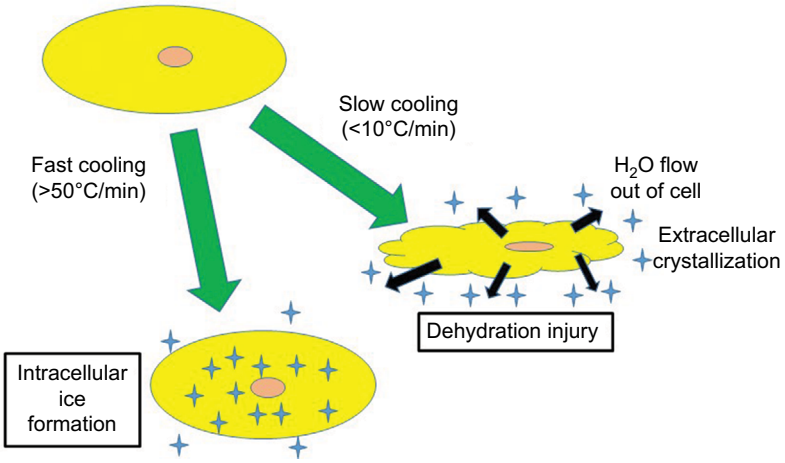

Figure 1 Cooling-induced cellular changes.

enable ablation of lesions (ie, benign, preinvasive, and malignant) and strictures within the gastrointestinal tract[12,13] and upper airways[14–16] by placing a cryocatheter into the working channel of an endoscope. The Company's proprietary, commercially available medical device, the truFreeze System® (CSA Medical, Lexington, MA, USA), employs a computer-driven method and apparatus to transport LN_2 from a Dewar inside the control console through a catheter and into a patient allowing LN_2 to be sprayed directly on the targeted tissue.[17] The sprayed LN_2, at a temperature of −196°C, impacts tissue and produces a flash freezing of the lesion with the formation of intracellular ice crystals (Figure 1) before cellular dehydration can occur.[18] These ice crystals further aggregate during the recovery (thawing) phase disrupting intracellular organelles such as mitochondria and endoplasmic reticulum while leaving the cell wall intact. The disruption of these energy-producing organelles leads to cell death. The ablated dead cells lose their cellular attachments or become apoptotic and are either reabsorbed, disintegrate, or "sluff-off" of the membrane wall, thus exiting the body. Following LN_2 spray procedures, healing follows in a rejuvenative fashion with minimal or no scarring.

In stark contrast are the heat ablation modalities such as radiofrequency, Bovie cautery, laser, and argon plasma coagulation. These ablation applications cause thermal fixation of tissue, a process of cellular and protein denaturation, leading to cell wall breakdown causing exposure of intracellular proteins to the immune system and leading to a reparative healing, the hallmark of which is fibrotic scarring.[19]

As is typical of an ablative cryosurgical tool, the truFreeze System allows the physician to determine the rate and total duration of cryogen delivery. The physician decides on the length of time that the cryogen be applied based on the characteristics of the abnormal tissue to be addressed.

CSA Medical Inc. is continuing to advance the application of the rejuvenative effects of LN_2 within various medical applications such as the use of a radial spray within lumens such as the airways or esophagus. In order to effectively ablate and potentially treat specific benign or malignant diseases or tissues, a predetermined and consistent amount of circumferential LN_2 cryogen spray must be delivered to the targeted areas within the patient's airway or esophagus that provides cryogenic ablation and healing effects in a safe and efficacious manner. This LN_2 spray approach is branded "Metered Cryospray™" (MCS). The following sections of this article describe the overall considerations of the MCS approach, test methods and results, and specific anatomical considerations of MCS.

MCS technical considerations

Development approach

The development phase of MCS was structured around the establishment of test fixtures and methods to evaluate the MCS cooling performance. This process followed a four-step methodology (Figure 2). First, numerical modeling was used to approximate the effect of MCS on human tissue and tissue mimetic gels including ballistic gels and high-temperature nontoxic (HTNT) gels. HTNT gel is a hydrogel consisting of water, sorbitol, starch, disodium phosphate, and iota carrageenan, which has been designed to melt at a temperature significantly above 37°C required to simulate human body temperature. The model was developed by using properties obtained from literature,[20,21] as well as differential scanning calorimetry (DSC) and thermal conductivity measurement of mucosal tissue and the gel mimetics in both frozen and unfrozen states. Then, gels were used to visually determine the appropriate radial head configuration that would produce a uniform spray with a circumferential effect over a range of

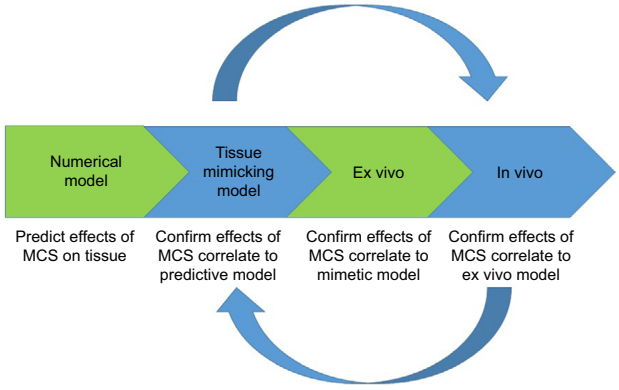

Figure 2 Gels and test fixture process.
Abbreviation: MCS, Metered Cryospray™.

lumen diameters. This spray distribution was evaluated by using phase Doppler particle analyzer (PDPA) and a LaVision laser sheet imager. Then, a more focused effort to establish the material properties of the gels and test fixture hardware and methods was made for quick system evaluations. These gel-based test fixtures revealed the need for further control of the cryogen delivery, including bench simulation of an in vivo bronchoscope using a heated water jacket in order to simulate more closely the anticipated treatment conditions. Data from these bench tests led to the incorporation of a catheter-mounted thermocouple and development of a temperature-driven control algorithm. Additional testing and modeling was necessary to establish a correlation between the gels and in vivo use of MCS. A porcine luminal model (bronchial airway lumen) was the chosen in vivo model, given the ability to access these lumens with a conventional bronchoscope.

Significant accomplishments were establishing cryospray parameters in gel studies and then confirming the tissue effects with pathology results from animal studies. A key process to establish the correlation of test stand measurements of gel with animal pathology was the use of viability staining[19,22] that would identify the cryoablated intact dead cells in a recently-treated extirpated animal tissue. Correlation was then facilitated by using a transient numerical heat transfer model (two-phase, with melting/solidification) exhibiting measured temperature-dependent gel thermal properties (ie, conductivity, density, and specific heat), gel fixture geometry, and measured thermal properties of porcine mucosal tissue. Given the thermal mapping data obtained during sprays in gel, the surface heat transfer properties are inferred for the proxy and then applied to a numerical model incorporating the geometry and properties of the porcine tissue. Model validation was accepted when the results of the porcine model matched the known injury depth (associated with the −20°C isotherm) for a given spray duration and intensity.

When the correlation between gel and bronchial tissue was established, the length of injury, depth of injury (DOI), and uniformity of radial pattern leading to circumferential LN_2 distribution were evaluated. As noted, the overall goal was to demonstrate that MCS achieved a consistent, uniformly radial LN_2 spray in lumens of varying diameters and lengths, resulting in DOIs within depth ranges anticipated by in vitro gel models. A series of HTNT gel tests were performed for several lumen sizes that are found to occur in animal and human airways: 6, 8, 12, and 18 mm. The purpose of this study was to evaluate centered LN_2 sprays and the resulting overall DOI in order to confirm temperature regimes for various acute animal studies. The catheter thermocouple temperatures were adjusted until the resulting DOI fits within the boundaries of a 0.1–0.5 mm DOI based on the established correlation between HTNT gel and porcine bronchial tissue (demonstrated with viability staining).

Numerical modeling

In order to understand the relevance of temperatures generated in HTNT gel test fixtures in predicting the amount of LN_2 that would be necessary to ablate human tissue to a specific depth, the thermal characteristics of our porcine model bronchial-wall human tissue proxy and our HTNT gel model had to be determined. After obtaining porcine bronchial tissue from a recently slaughtered pig from a local meat packing house (Blood Farm, West Groton, MA, USA), the bronchial epithelium was dissected from the cartilage wall. This tissue specimen along with a representative sample of HTNT gel was sent for analysis to Analytical Answers, Inc. (Woburn, MA, USA), who studied the thermal properties of both samples by using DSC per ASTM E1269.

Then, a two-dimensional axisymmetric thermal fluid model in COMSOL,[23] a finite element analysis software package, was developed. From this work, two models were created, one for human bronchial tissue using the data gathered by testing the thermal properties of porcine bronchial tissue (Table 1) and the second for HTNT gel (Table 2). A convective heat flow model was used as the surface boundary condition at the lumen interior. The tissue was modeled by using Penne's equation and includes latent heat associated with phase change and crystallization as well as the metabolic rate and the perfusion rate. The gel was modeled as a solid with temperature-dependent properties and phase change. MCS was then delivered to the surface of HTNT gel embedded with thermocouples at specific depths (ie, 0.25,

Table 1 Thermal property data for porcine tracheal mucosa (Analytical Answers, Inc., Woburn, MA, USA)

Property	Value	Units	Tolerance
Melt/solidification temperature	3.5	°C	±1.5
Latent heat of fusion	207	J/g	±4
Crystallization temperature	−14	°C	±1
Latent heat of crystallization	−96	J/g	±10
Specific heat capacity at 20°C	3.85	J/g-K	±0.2
Specific heat capacity at −20°C	1.92	J/g-K	±0.06
Thermal conductivity at 20°C	0.453	W/m-K	±0.05
Thermal conductivity at −170°C	1.619	W/m-K	±0.85
Density	1050	kg/m^3	±10

Table 2 Thermal property data for high-temperature nontoxic (HTNT) gel (Analytical Answers, Inc., Woburn, MA, USA)

Property	Value	Units	Tolerance
Melt/solidification temperature	−1.82	°C	±0.1
Latent heat of fusion	142	J/g	±9
Crystallization temperature	−18.5	°C	±0.3
Latent heat of crystallization	141	J/g	±4
Specific heat capacity at 20°C	6.76	J/g-K	±0.03
Specific heat capacity at −20°C	4.05	J/g-K	±0.01
Thermal conductivity at 25°C	0.624	W/m-K	±0.06
Thermal conductivity at −170°C	1.083	W/m-K	±0.03

0.70, and 2.0 mm) in a 3 mm thick wall. The temperatures obtained from these thermocouples embedded in HTNT gel were interpreted by using the models to predict the depth of thermal penetration that would occur in bronchial wall tissue.

Establishing radial head geometry

It is desirable to use a single radial pattern in order to uniformly generate an outwardly directed radial LN_2 spray onto the walls of lumens of varying diameters. However, for lumens with large diameter and length such as those found in the esophagus or trachea, a multirow design was determined to be more effective in producing uniform and consistent LN_2 sprays. An evaluation of a variety (Figure 3) of catheter hole patterns in the tip was conducted to characterize spray outputs. The test matrix included two LN_2 sprays each in lumen phantoms of three inner diameters constructed of ballistic gel to visualize freeze zones (including radial uniformity and depth and length of freeze zone); measurements of flow rates and power delivered over a series of three LN_2 sprays using specific test fixtures; and measurements of the rate of temperature change of the lumens, evenness of spray, and the final temperature achieved.

Figure 3 Hole patterns tested for spray capabilities.

Figure 4 shows the results of one of the set of tests performed in an 18 mm lumen (used as a reference point for one of the largest airway lumen diameters that would be medically relevant) for one of the hole pattern configurations. This sample generated a uniform circumferential freeze zone in the various quadrants in all relevant lumen diameters. Other samples did not achieve the same uniform spray results.

For measurements of spray evenness around lumen circumference, the rate of temperature change, and the final temperature achieved, lumens were configured with between four and 240 ultrafine thermocouples (0.0025 cm diameter) in selected locations (Figure 5). Each lumen was sprayed using the same 25s spray time, repeated three times for confirmation of repeatability. This length of time was chosen as it allowed for detectable thermal penetration into the gel, no matter the lumen diameter. Figure 6 shows a typical testing result. One notes that a high degree of consistency was observed in the thermal profile for each of the thermocouple units.

Upon completion of the testing, a finite element analysis of the most favorable designs was conducted to determine the most robust solution. Figure 7 shows a typical mesh pattern

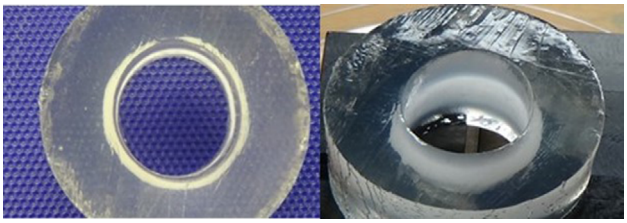

Figure 4 Freeze zone determinations in ballistic gel for LN_2 spray testing.

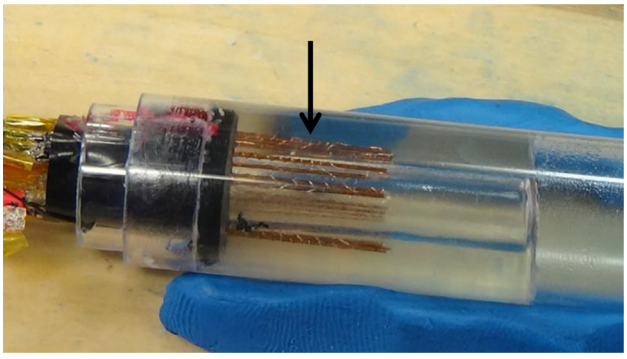

Figure 5 Test structure with multiple thermocouples (black arrow) embedded in gel.

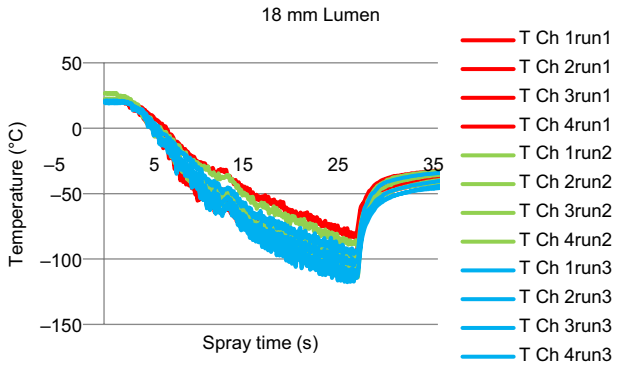

Figure 6 Temperatures as a function of spray time for 18 mm lumen diameter (T Ch refers to each embedded thermocouple).

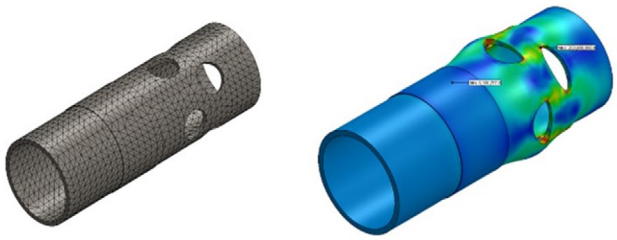

Figure 7 Mesh and stress simulation for test radial pattern.

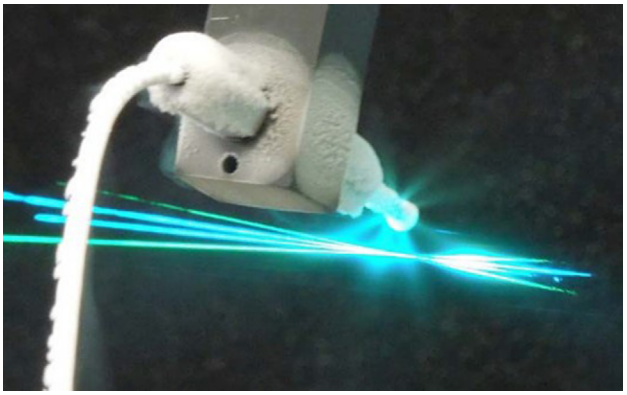

Figure 8 Phase Doppler particle analyzer measurement of catheter spray output.

and simulation of stresses. Given that this catheter enters the body via the working channel of an endoscope, consideration of the maximal scope insertion force applied at the distal face was used to simulate the greatest axial compression. Determination of the von Mises stress and maximal displacements were completed, and the most robust of the various patterns was selected.

Spray characterization testing

In order to more fully understand the LN_2 spray conditions, additional characterization tests were performed. In particular, a PDPA and a LaVision laser sheet imager were employed to provide more detailed data on the spray characteristics. These tests were performed at Spray Analysis and Research Services (Spraying Systems Co., Wheaton, IL, USA) and encompassed both open end spray and radial spray catheters.

A PDPA (TSI Inc., Shoreview, MN, USA) provides data on spray drop sizes and velocity distributions by taking point measurements at multiple locations within a spray plume. With the test apparatus, the laser point size is a few microns in diameter, and the point must traverse across the edges of the spray plume to capture data on the plume size edge-to-edge, drop sizes at each position about the plume, and velocity at each of the points evaluated. Figure 8 shows an image taken during testing with a radial spray catheter.

Two distances, selected to closely match the existing human lumen diameters of 7.8 and 9.8 mm, were used in order to capture the full extent of the spray profile. The edges of the spray were determined by examining a decrease in both drop velocity and the number of drops observed. Typically, at the edge of the spray, the data rate is reduced from >10,000 drops in a 30s period to ~500 drops over the same time period.

The PDPA examined $D_{V0.1}$, $D_{V0.5}$, $D_{V0.9}$, and D_{32} diameters where these parameters are a means of expressing drop size in terms of the volume of LN_2 sprayed (Table 3). $D_{V0.1}$ is the value where 10% of the total volume (or mass) of LN_2 sprayed is made up of drops with diameters smaller than or equal to this value; $D_{V0.5}$ is the median volume diameter where 50% of the total volume of LN_2 sprayed is made up of drops with diameters larger than the median value and 50% smaller than the median value; and $D_{V0.9}$ is where 90% of the volume of LN_2 sprayed is made up of drops with diameters smaller than or equal to this value. D_{32} is the Sauter mean diameter and is a means of expressing the fineness of a spray in terms of the surface area produced by the spray. It is the diameter of a drop having the same volume-to-surface area ratio as the total volume of all the drops to the total surface area of all of the drops.

There is a significant reduction in velocity and overall drop size between the straight spray catheter and the radial spray catheters. This is due to the effects of shear in the catheter as the LN_2 abruptly changes direction right before exit. These measurements demonstrated that the radial spray catheter provides a more diffused and controlled spray, and thus, it is expected to be able to more effectively spray more delicate areas of the body with lumens of smaller diameter.

Figure 9 shows the average drop diameter ($D_{V0.5}$) for the end spray catheter at various points across the spray plume for two different test runs. The shape and overlay of the runs demonstrate excellent repeatability. It is also

Table 3 Phase Doppler particle analyzer results of drop size for various catheter types

Catheter type	Liquid pressure (psi)	Spray height (mm)	$D_{v0.1}$ (μm)	D_{32} (μm)	$D_{v0.5}$ (μm)	$D_{v0.9}$ (μm)	Average velocity (m/sec)
Straight orifice open end	19	8	48	79	91	155	115
			44	65	85	148	115
Offset radial orifice	19	4	32	55	65	121	25
			33	57	67	124	23
In–line radial orifice	19	3	34	60	73	136	23

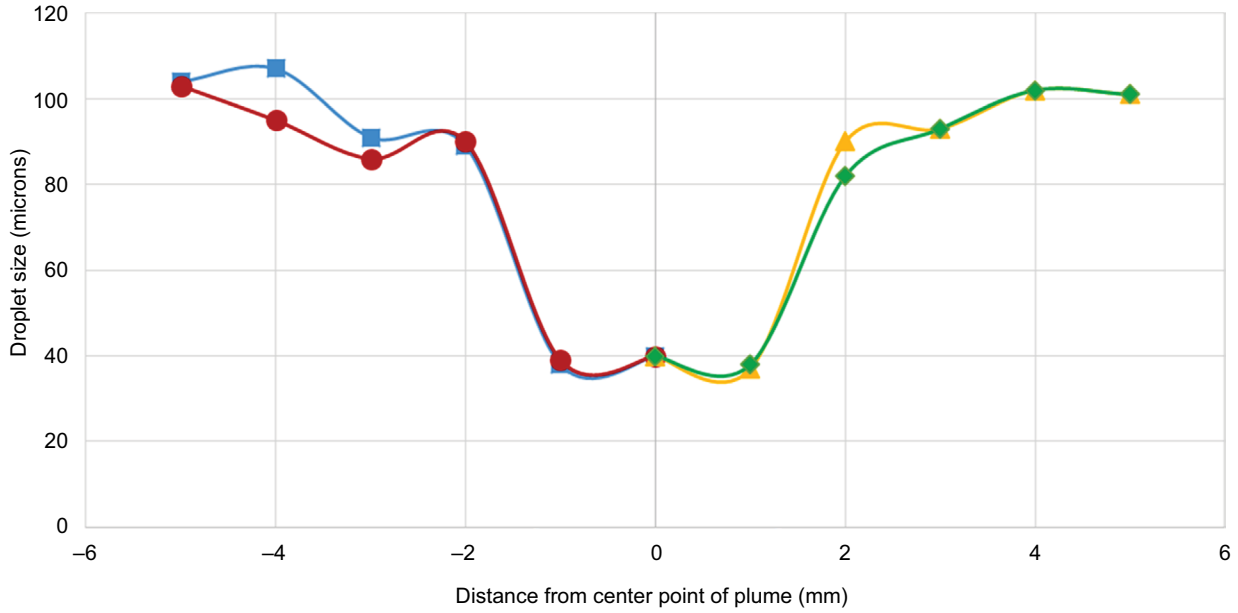

Figure 9 Open-end catheter droplet size ($D_{v0.5}$) across spray plume.
Notes: Blue (square data points)/green (diamonds) are Spray 1; red (circles)/yellow (triangles) are Spray 2.

interesting to note that the general shape of this graph, with smaller drops occurring near the center and larger drops occurring near the edges, is the opposite of what would be expected from a full-cone, narrow-angle hydraulic nozzle spraying water. Water would exhibit larger drops in the center of the nozzle and smaller drops at the edges. However, this graph is consistent with a multiphase flow in which the core is high-speed gas and the annulus is slow-moving/wetted liquid. The small droplets at the center are fine mist particles as an artifact of the flow regime. The large annulus of droplets is caused by the natural breakup of the exiting liquid content near the walls. This characteristic of spray may be ideal for LN_2 cryospray ablation as it distributes the freezing power more evenly across the spray as in an annulus.

Laser sheet imaging (LSI) was conducted by using a LaVision SprayMaster system to obtain qualitative and quantitative visualization of the LN_2 spray process. This integrated imaging system uses a laser sheet to simultaneously measure the intensity of the individual spray plumes radiating from each of the radial head openings. Laser light sheets slice through the plume with high temporal and spatial resolution. The approach helps to determine the spray concentration distribution and focuses on the size, shape, and relative distribution of the spray plume to provide two-dimensional (planar cross section) spray concentration results. Figure 10 shows one of the sets of images obtained from a radial spray catheter that was oriented to spray vertically downward so the laser sheets describe a plane that cuts through an axial position centered on one of the two rows of holes in the catheter tip. As may be noted, the image shows a very radially symmetric LN_2 spray (in both patterning and intensity) with a clear differentiation between the centers of the spray plumes from the forward and rear offset catheter holes.

These combined (PDPA and LSI) tests provided useful data on the characteristics of the LN_2 sprays for various catheter configurations to guide selection of the optimum variant for the radial spray catheter to be used in further preclinical

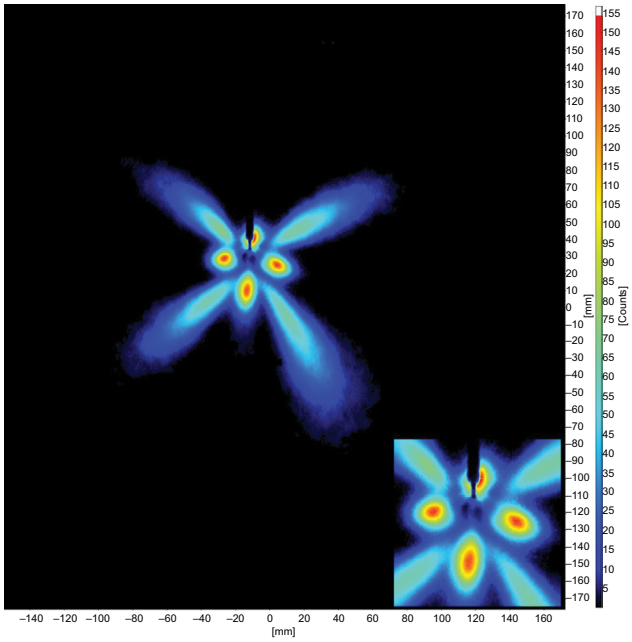

Figure 10 Radial catheter laser sheet imaging showing droplet counts as a function of position (inset image in lower right corner shows enlarged center pattern image. Inset scale not shown).

and clinical studies. In particular, these tests demonstrate that the radial design generates consistent, even, and overlapping annular plumes that result in a smooth circumferential effect in cylindrical lumens.

Core probe and cavity pressure test fixtures

A measurement system that is repeatable and reproducible for the purpose of evaluating LN_2 cryospray output was required for design verification testing. This type of measurement system made it possible to evaluate part-to-part variation of components with the confidence necessary to ensure data consistency and stability. A core probe fixture and a cavity pressure fixture were designed to measure the total cryogen delivery performance (defined as total cooling energy output of the system as controlled by using the MCS time and temperature conditions) and the resulting pressure built during a cryospray from LN_2 to N_2 conversion, respectively. Figure 11 shows a schematic diagram of the core probe and a photograph of a nominal test setup. The core probe includes a cylindrical body of known mass and heat transfer properties with a thermocouple that is thermally bonded to the mass to measure total energy transmitted to the probe during an LN_2 spray. The catheter (typically used in the working channel of an endoscope) is mounted within a heated water jacket (37°C) to simulate LN_2 spraying in a body cavity.

Figure 12 shows a schematic representation of the cavity pressure test fixture. This device consists of a known volume with metering valve and pressure transducer to determine the cavity pressure during controlled LN_2 spray that subsequently transitions into N_2 gas. This method allowed an evaluation of the N_2 gas pressure generated with LN_2 sprays to use as a proxy of pressure to assess the most stressful conditions that may arise during in vivo human use. These tests confirmed that the maximum cavity pressure remained below 40 cm H_2O for metered cryosprays of <25 s and demonstrated that, for pressure considerations, MCS may be used safely in esophageal or airway lumens in humans.[24]

Porcine animal model testing

Throughout the development of MCS, the results noted in HTNT gel studies were measured against findings from in vivo testing in the porcine animal model. In order to determine the depth to which the cryothermic ablation effect penetrated the bronchial airway wall, viability staining was applied on bronchial tissue extirpated after treatment. Viability staining is based on the principle that regions of thermal tissue necrosis may be identified by using a reaction that converts a colorless salt to a colored formazan pigment within viable tissues. There are two compounds used for this process: 1) triphenyltetrazolium chloride (TTC), and 2) nitro blue tetrazolium (NBT). Both these compounds use the dehydrogenase enzyme cofactor reaction to enact a full color change with viable tissues (colorless to red maroon with TTC and colorless to blue-black with NBT) or a partial color change in mixed viability tissues (colorless to pink with TTC and colorless to grey with NBT). Nonviable or necrotic tissues that lack intact enzymatic activity to metabolize the salts do not stain. TTC staining is optimally used macroscopically to detect thermal necrosis and its boundary with viable tissues. NBT staining is optimally used to microscopically detect thermal necrosis and its boundary with viable tissues.[19,22] Figure 13 shows a comparison of normal and cryospray-treated tissues visualized with NBT staining.

A series of short-term survival (<1 h after the completion of MCS treatment in vivo to euthanasia and tissue extirpation) porcine animal studies were evaluated at the completion of the design phase using final MCS control parameters. Terminal temperatures governed the amount of spray used in relationship with the diameter of the measured airways (Figure 14) and led to adequate depths of tissue ablation providing in vivo confirmation of the data generated from test fixtures.

Moreover, animal testing also identified a potential variable (mucus or other fluids within the working channel

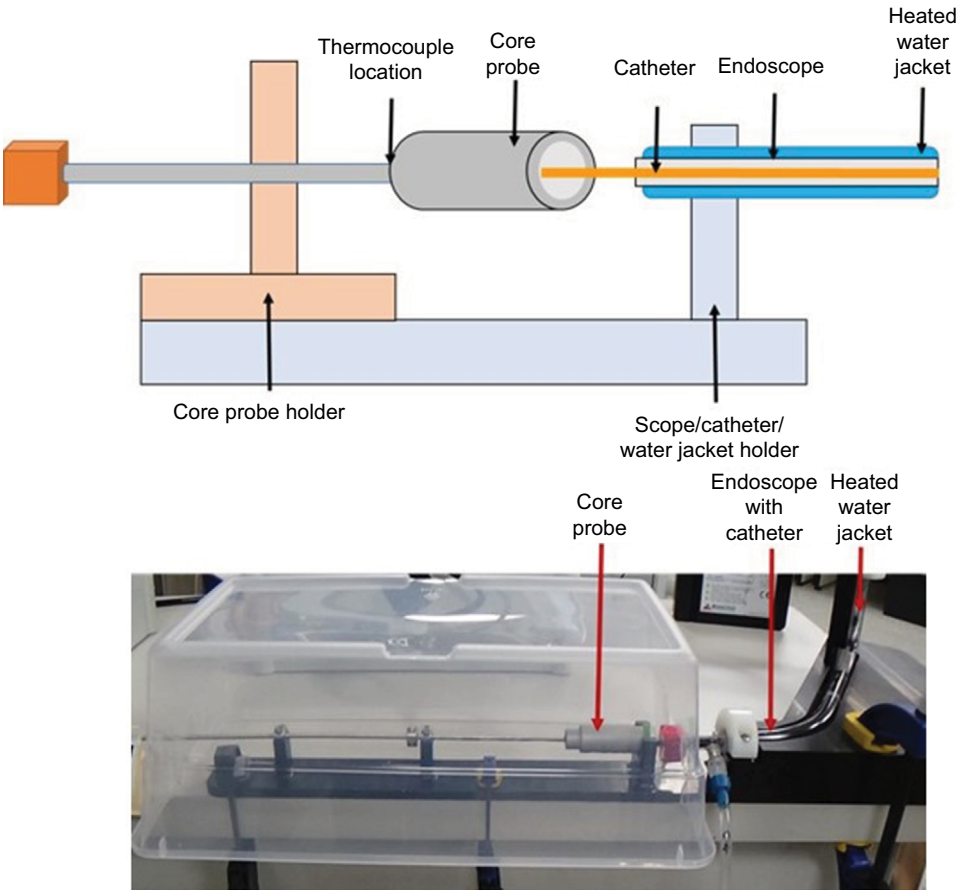

Figure 11 Core probe measurement system to determine LN_2 cryospray output.

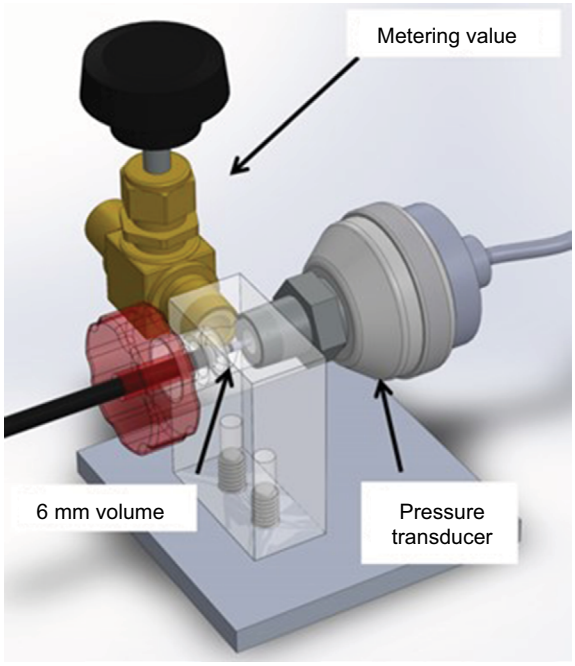

Figure 12 Schematic of cavity test fixture for a 6 mm lumen diameter.

of the endoscope is a source of change in flow enthalpy during a cryospray) that could affect the MCS control algorithm by delaying the time to reach the minimum target temperature (as measured by the thermocouple on the catheter). With the inclusion of a maximum time limit coupled with empirically selected bounding conditions (slope and R^2 value of a linear curve fit of the catheter thermocouple temperature data), metered cryosprays with excessive amounts of material in the bronchoscope working channel are automatically detected and terminated, prompting user intervention. A scope cleaning technique was demonstrated to be an effective means of removing excessive amounts of material from the endoscope, facilitating subsequent successful sprays.

Despite some variation in pathological findings due to the sectioning method, many LN_2 cryosprayed sections revealed circumferential to nearly circumferential effect to the optimal target depth range of 0.1–0.5 mm in porcine airways by using the final empirically developed MCS

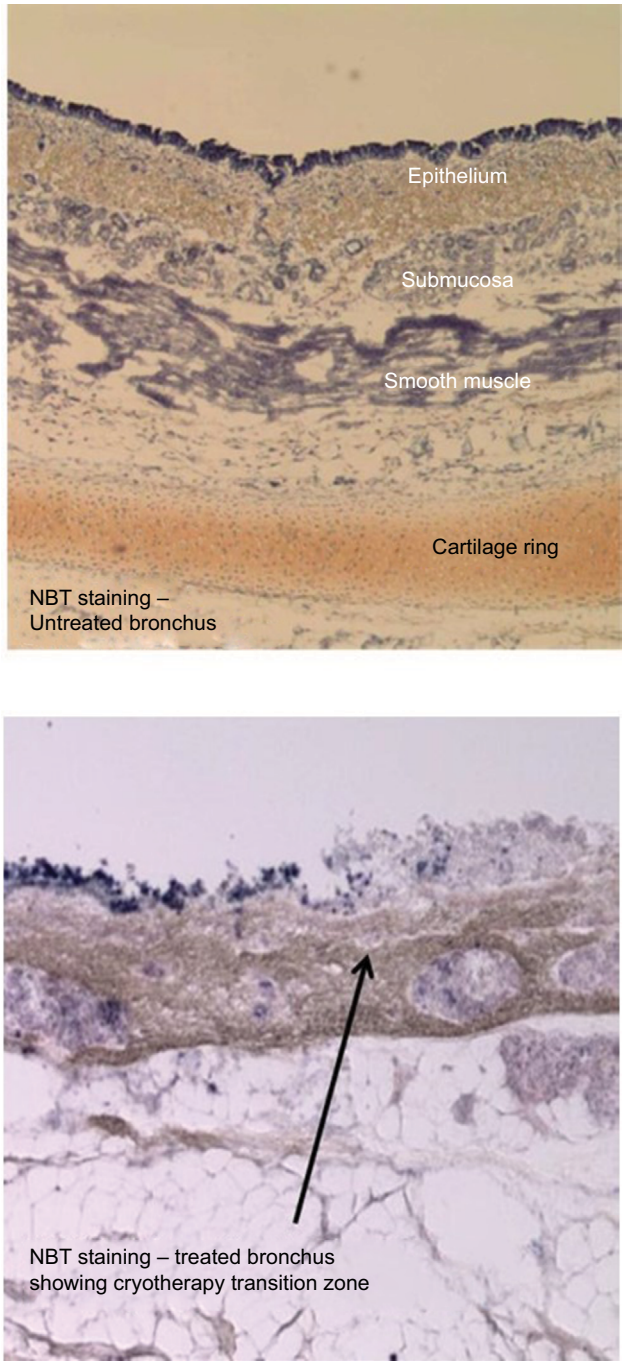

Figure 13 NBT stain identifies cryothermic effects by staining nontreated cells (dark blue), whereas treated cells remain unstained.
Note: Stain changes color based on viable cell energy production.[19,22]
Abbreviation: NBT, nitro blue tetrazolium.

treatment protocol. In total, five confirmatory acute animal studies were performed confirming the tissue depth of treatment (Figure 15).

Catheter temperature correlation

A series of tests were completed to determine the correlation of the catheter temperature with catheter energy output as this would allow for a repeatable and controlled application of LN_2 spray. The thermocouple that was affixed to the catheter at the distal end was used to measure the catheter temperature as a function of spray time and lumen size. These measurements demonstrated that there was a strong, direct relationship between the terminal temperature (ie, the net energy removal from the stainless catheter wall) and the amount of LN_2 delivered to targeted ablation areas. Figure 14 shows the relationship of lumen diameter with catheter terminal temperature. The selected terminal temperatures and the cooling rate of change as measured by the catheter thermocouple caused a desired effect in porcine bronchial tissue as a result of cooling delivery performance (energy output).

When the control algorithm was established, the length of injury, DOI, and uniformity of radial pattern distribution were evaluated. As noted, the overall goal was to demonstrate that MCS achieved a consistent, uniform, radial LN_2 spray in lumens of varying diameters and lengths, resulting in DOIs circumferentially within anticipated ranges (for development purposes, a target DOI range of 0.1–0.5 mm was used; however, the control system can be adjusted to achieve any DOI determined to be clinically required, within the limits of the cryogen delivery). A series of HTNT gel tests were performed for several lumen sizes: 6, 8, 12, and 18 mm. The purpose of this study was to evaluate centered LN_2 sprays and the resulting overall DOI in order to confirm terminal catheter temperature settings for various acute animal studies. The catheter thermocouple termination temperatures were adjusted until the resulting DOI fits within the boundaries of 0.1–0.5 mm based on the established correlation between HTNT gel and porcine bronchial tissue (demonstrated with viability staining). Figure 16 displays the resulting minimum HTNT gel temperature at 0.25 mm as a function of spray duration. The polynomial curve fits in Figure 16 correspond to lethal isotherms (−20°C) in tissue at the indicated depths, as determined by using correlated numerical modeling.

By using ballistic gel, a complementary series of tests with varying lumen sizes was completed to determine the length of the injury resulting from an LN_2 MCS. Table 4 shows the results.

A further series of HTNT gel tests were performed to evaluate the overall length of injury at various nominal depths for centered sprays in relation to other variables. The following conditions were evaluated:

1. Off-center catheter: half the distance from center to luminal wall (expected variation in clinical use);

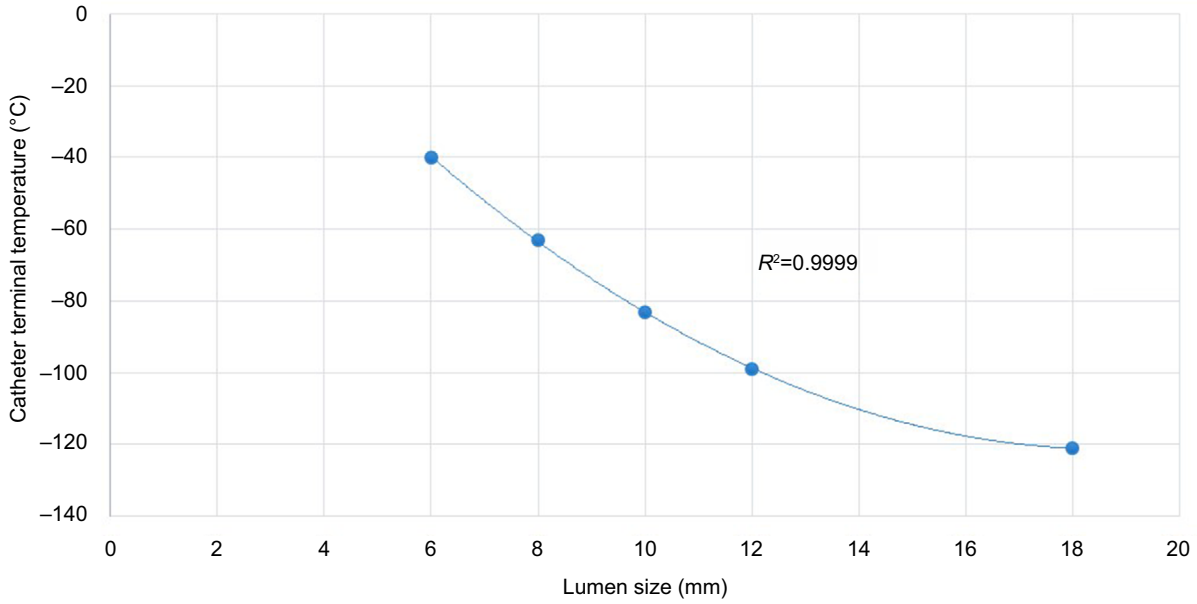

Figure 14 Catheter terminal temperature versus lumen size.

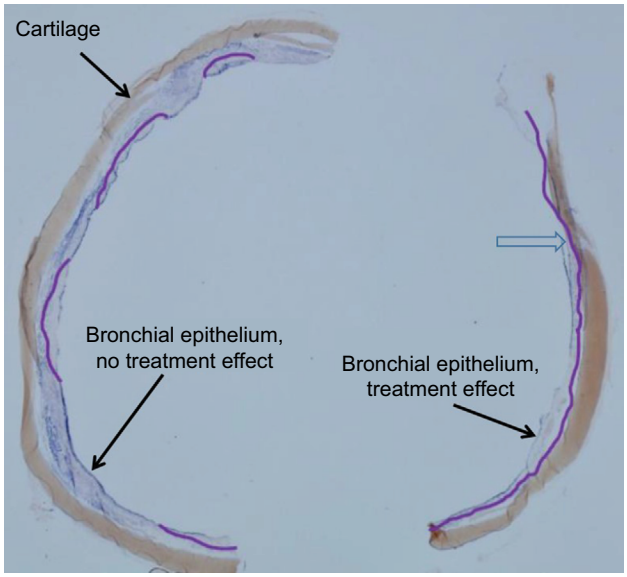

Figure 15 Representative porcine model distal trachea.
Note: Purple line (open arrow) depicts essentially circumferential MCS treatment effect.
Abbreviation: MCS, Metered Cryospray™.

2. Off-center catheter: 1 mm from the luminal wall (worst-case scenario);
3. 2X overdose of LN_2 spray (misuse and/or exaggerated anatomical variation);
4. Temperature for low-energy limit;
5. Maximum time cutoff;
6. Two sprays with 1 cm pull-back in an 8 mm lumen.

The lengths and DOIs were measured for each of these clinically relevant challenge conditions. Figure 17 shows a representative result for an 8 mm lumen diameter.

Spray effects were evaluated by using perfect and nonperfect use conditions with the catheter centered in the lumen and conditions that simulate the anticipated variation of clinical use such as the catheter off-center in the lumen and variation in lumen diameter (Figure 18). As observed, with off-center catheter positioning, the temperature distribution profile still produces a circumferential DOI within desired parameters.

The gel testing and animal testing were an iterative process that established the relationships between the two methods. The outcome yielded the MCS parameters required to inform an algorithm that would deliver a controlled and uniform amount of LN_2 at desired depths in tissue. MCS automatically delivers an appropriate amount of LN_2 spray as a function of lumen diameter, based on a maximum spray time or a threshold catheter temperature, whichever comes first.

Summary

This article summarizes the development of a novel cryospray system that delivers a controlled, disease- or tissue-specific, and repetitively consistent radial spray of LN_2 through a catheter delivered into the human body through the working channel of an endoscope. Unlike cryoprobes or external topical LN_2 spray used for general tissue ablation, this system could be used to apply LN_2 cryospray for specific disease conditions as well as for ablation of unwanted tissue. The basis of the process is the regenerative or rejuvenative healing that results from flash-freeze LN_2 cryogenic ablation.

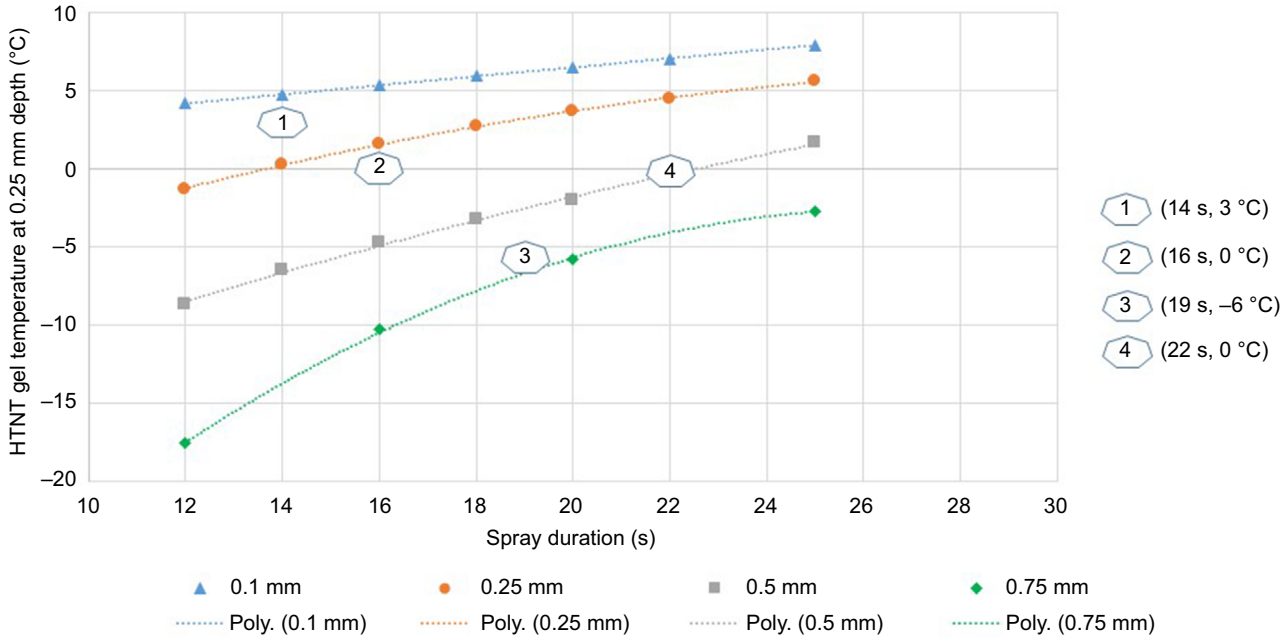

Figure 16 Correlation of HTNT gel temperatures with DOI.
Notes: The DOI is determined by looking at the contour lines. For example, the "1" data point (a 14s spray with a gel temperature of 3°C) falls between the 0.1 and 0.25 mm DOI lines; therefore, in a human, it would be expected to see a DOI between 0.1 and 0.25 mm. The "2" data point is a DOI between 0.25 and 0.5 mm. The "3" data point falls between 0.5 and 0.75 mm, and the "4" data point is on the line at 0.5 mm.
Abbreviations: DOI, depth of injury; HTNT, high-temperature nontoxic; Poly., polynomial fit.

Table 4 Ballistic gel length of injury measurements

Lumen diameter (mm)	Approximate length of injury (mm)
6	4–6
8	5–7
10	7
12	7–8
18	9–12

In order to address specific disease conditions, the LN_2 cryospray process requires novel controls to ensure that the amount delivered is indeed consistent. The ability to correlate the temperature trace of a thermocouple located on the distal end of the spray catheter to the intended cryothermic tissue treatment was the key to achieve cryospray control, a process that has been identified as MCS. This development required first comparing and modeling the thermal characteristics of targeted human tissue to gel-based test fixtures. Such a process allowed for interpretation of data generated from subsequent gel-based test fixtures and core probes. This correlation was carried through the development process.

Safe egress of the nitrogen gas generated during the state transition of LN_2 from the internal organ system being sprayed with LN_2 is essential. Modeling the gas pressure developed within an organ during spray cryotherapy and its evacuation is essential for a safe LN_2 application process. Through specific test fixtures and analysis of gas egress patterns, safe LN_2 cryospray methods have been determined such that the nitrogen gas generated during MCS egresses safely from the target organ.

The depth of cryoablation in a specific organ to produce the desired effect on the abnormal epithelial lining will be defined by the disease process. The gel and core-probe test fixtures enable predictions of the amount of MCS and to subsequently document the in vivo tissue effect using a porcine animal model. This tissue model requires the use of a special tissue staining process that identifies cell layers that have been ablated due to the inability of cryo-treated cells to generate energy. These viability stains change from clear to specific color within cells that are still viable and energy-producing, whereas the intact nonviable cells do not stain. Such animal studies are the final proxy for the anticipated in vivo human effect from MCS.

The test proxies noted in this report support the thoughtful and methodical development of safe use of this approach.

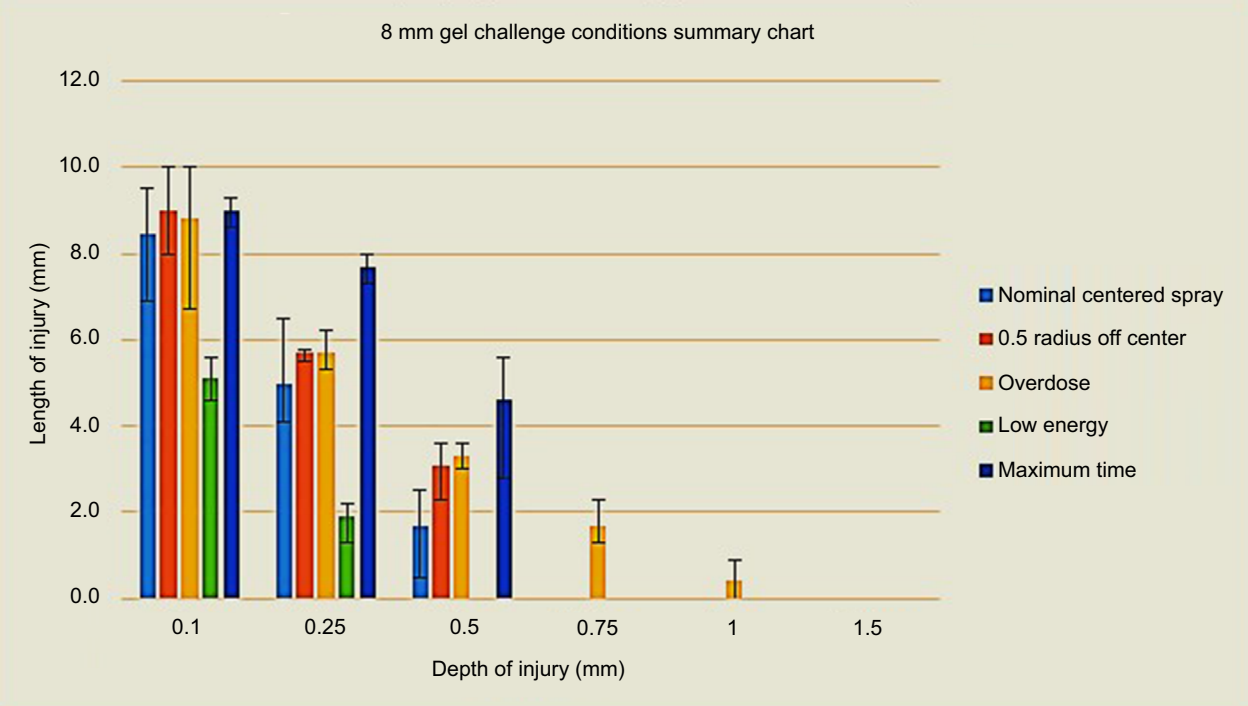

Figure 17 Length of injury measurements of MCS in an 8 mm diameter of HTNT gel.
Abbreviations: HTNT, high-temperature nontoxic; MCS, Metered Cryospray™.

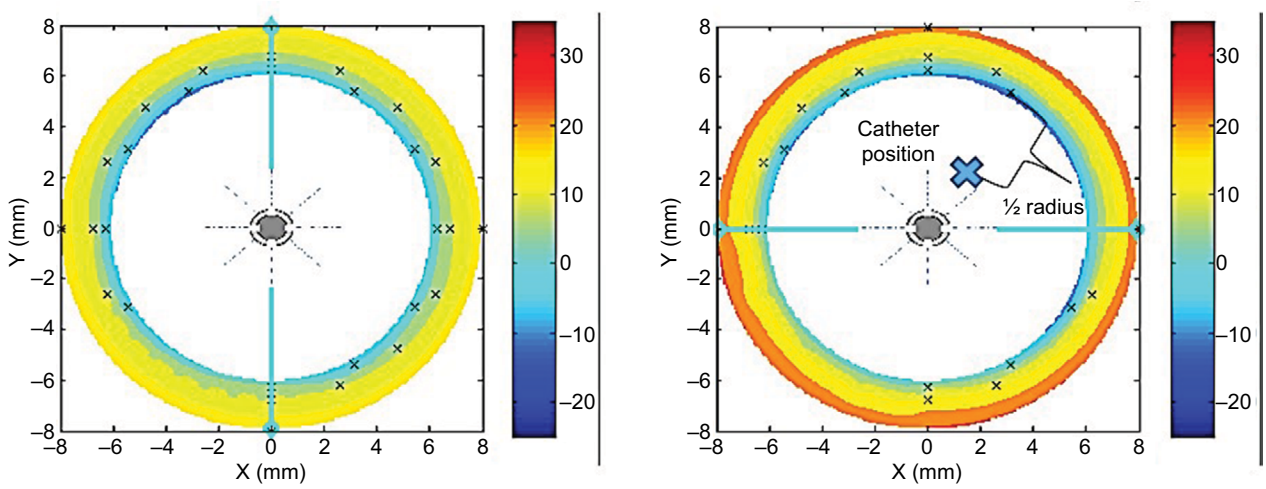

Figure 18 Centered spray (left) and off-center spray (right) final temperature profiles in HTNT gel with a 12 mm lumen.
Notes: Actual catheter position is denoted with a bold X. Small x markers indicate locations of embedded thermocouples on rings of 0.25, 0.75, and 3 mm depth relative to the lumen surface. Color scales are in °C.
Abbreviation: HTNT, high-temperature nontoxic.

Acknowledgments

The authors wish to thank the team at CSA Medical Inc. for their efforts and support to make this work possible. The authors note that this work was fully funded by CSA Medical Inc.

Disclosure

All authors except James E Coad, MD, are employees of CSA Medical Inc. Dr Coad is a paid consultant of CSA Medical Inc. The authors report no other conflicts of interest in this work.

References

1. White CA. Liquid air in medicine and surgery. *M Rec*. 1899;56:109.
2. Pusey WA. Use of carbon dioxide snow in the treatment of nevi and other skin lesions. *JAMA*. 1907;49:1354.
3. Grimmett H. Liquid nitrogen therapy: histological observations. *Arch Dermatol*. 1961;83:563–567.
4. Zacarian SA, Adham MI. Cryogenic temperature studies of human skin. *J Invest Dermatol*. 1967;48:7–10.
5. Freiman A, Bouganim N. History of cryotherapy. *Dermatol Online J*. 2005;11(2):9. Available from: http://escholarship.org/uc/item/4f62h9vt. Accessed February 12, 2016.

6. Liapi E, Geschwind JF. Transcatheter and ablative therapeutic approaches for solid malignancies. *J Clin Oncol*. 2007;25(8):978–986.
7. Klatte T, Grubmüller B, Waldert M, Weibl P, Remzi M. Laparoscopic cryoablation versus partial nephrectomy for the treatment of small renal masses: systematic review and cumulative analysis of observational studies. *Eur Urol*. 2011;60(3):435–443.
8. Pantuck AJ, Zisman A, Cohen J, Belldegrun A. Cryosurgical ablation of renal tumors using 1.5-millimeter, ultrathin cryoprobes. *Urology*. 2002;59(1):1340–1343.
9. Galilmedical.com [homepage on the Internet]. Arden Hills, MN, USA. Available from: www.galilmedical.com/cryoablation-products/needles/. Accessed February 12, 2016.
10. Hendricks RC, Peller IC, Baron AK. *Joule-Thomson Inversion Curves and Related Coefficients for Several Simple Fluids*. NASA Technical Note D-7807. Washington, DC: NASA; 1972.
11. Ryan J. General guide for cryogenically storing animal cell cultures. Acton, MA: Corning Inc. Life Sciences; 2016. Available from: https://www.corning.com/media/worldwide/cls/documents/t_cryoanimalcc.pdf. Accessed February 12, 2016.
12. Greenwald BD, Dumot JA, Abrams JA, et al. Endoscopic spray cryotherapy for esophageal cancer; safety and efficacy. *GIE*. 2010;71:686–693.
13. Shaheen NJ, Greenwald BD, Peery AF, et al. Safety and efficacy of endoscopic spray cryotherapy for Barrett's esophagus with high-grade dysplasia. *GIE*. 2010;71:680–685.
14. Browning R, Parrish S, Sarkar S, Turner JF, Jr. First report of a novel liquid nitrogen adjustable flow spray cryotherapy (SCT) device in the bronchoscopic treatment of disease of the central trachea-bronchial airways. *J Thorac Dis*. 2013;5(3):E103–E106.
15. Fernando HC, Dekeratry D, Downie G, et al. Feasibility of spray cryotherapy and balloon dilation for non-malignant strictures of the airway. *Eur J Cardiothorac Surg*. 2011;40:1177–1180.
16. Krimsky WS, Rodriques MP, Malayaman N, Sarkar S. Spray cryotherapy for the treatment of glottic and subglottic stenosis. *Laryngoscope*. 2010;120:473–477.
17. Sachdeva A, Pickering EM, Lee HJ. From electrocautery, balloon dilation, neodymium-doped:yttrium-aluminum-garnet (Nd:YAG) laser to argon plasma coagulation and cryotherapy. *J Thoracic Dis*. 2015;7(S4):363–379.
18. Yiu W, Basco MT, Aruny JE, Cheng SWK, Sumpio BE. Cryosurgery: a review. *Int J Angiol*. 2007;16(1):1–6.
19. Coad JE. Practical pathology perspectives for minimally invasive hyperthermic medical devices. *Proc SPIE*. 2011;7901:1–12.
20. McIntosh RL, Anderson VA. A comprehensive tissue properties database provided for the thermal assessment of a human at rest. *Biophys Rev Lett*. 2010;5:129.
21. ITIS. Foundation for Research on Information Technologies in Society, Documentation v 2.4; 2013. Available from: www.itis.ethz.ch. Accessed July 30, 2013.
22. Rupp CC, Nagel TC, Swanlund DJ, Bischof JC, Coad JE. Cryothermic and hyperthermic treatments of human leiomyomata and adjacent myometrium and their implications for laparoscopic surgery. *J Am Assoc Gynecol Laparosc*. 2003;10:90–98.
23. COMSOL Multiphysics Simulation Environment (versions 4.4 & 5.0) 2015. Available from: COMSOL Inc., Burlington, MA, USA.
24. Barash PG, Cullen BF, Stoelting RK, Cahalan MK, Stock MC, editors. *Clinical Anesthesia*. 6th ed. Philadelphia: Lippincott, Williams & Wilkins; 2009:251.